# The development of an optimized and reliable iron overload HepG2 cell model

**Usama Abbasi**
University of British Columbia
**Srinivas Abbina**
University of British Columbia
**Jayachandran N. Kizhakkedathu** ( jay@pathology.ubc.ca )
University of British Columbia

**Article**

**Keywords:**

**Posted Date:** August 24th, 2022

**DOI:** https://doi.org/10.21203/rs.3.rs-1976449/v1

# Abstract

Cell-based iron overload models provide tremendous utility for the investigations into the pathogenesis of different diseases as well as assessing efficacy of various therapeutic strategies. In the literature, establishing such models vary tremendously with regards to cell lines, iron source, iron treatment conditions and duration. Due to this diversity, researchers reported significant differences in the measured outcomes, either in cellular function or response to a stimulus. Herein, we report the process required to establish an iron overload HepG2 cell model to achieve a consistent and reproducible results such that the literature can strive towards a consensus. Iron loading in cells was achieved with 50 μM of iron every 24 hours for 2 days, followed by an additional 24 hours of maintenance in fresh media. We demonstrated that iron overloaded cells had significantly increased ROS generation, labile and total iron whilst having various cellular functions resemble cells without iron overload. The present report addresses key pitfalls with regards to the lack of consensus currently present in the literature.


# Introduction

Iron is an essential mineral for all eukaryotes; it serves as a prosthetic group for a variety of proteins involved in central cellular processes.[1–3] As such, vertebrates have evolved highly specialized mechanisms that tightly regulate iron uptake, transport and utilization, recycling, and storage. The liver plays a central role in coordinating iron homeostasis; all acquired iron enters the liver, 80% of which are comprised of hepatocytes,[4,5] where it is either stored or utilized intracellularly, or mobilized for systemic demands.[6] Approximately, 30% of the total amount iron is stored in the liver.[7,8] A perturbance in iron homeostasis can result in iron overload either through genetic disorders that give rise to hereditary hemochromatosis, or acquired as a result of another disease (including thalassemia, acquired anemia, myelodysplastic syndromes and dysmetabolic iron overload syndrome) that give rise to secondary hemochromatosis with excess liver iron.[6,9,10] Moreover, excess free iron is directly correlated to hepatic tissue injury, giving rise to hepatic insulin resistance,[11,12] fibrosis and cirrhosis,[13,14] and increased risk for hepatocellular carcinoma.[15,16]

Acquired iron, either transferrin-bound iron (TBI) or non-transferrin bound iron (NTBI) under pathological conditions, enters a transient pool of redox-active iron referred to as the labile iron pool (LIP).[17–20] This metabolically active iron serves as a cross-roads of metabolic pathways.[19] In diseases states, where there is elevated labile iron, toxicity ensues through the generation of reactive oxygen species (ROS) *via* the Haber-Weiss reaction, which imparts oxidative damage to lipids, proteins, and DNA.[21–23] Ultimately, these events disrupt vital metabolic functions leading to cell cycle arrest, apoptosis and necrosis.[24,25] Thus, it is important to have a reliable and reproducible iron overload model to study biology and evaluate therapeutics.

Although, there are numerous investigations describing the effect of hepatic iron overload on various cellular functions in the context of different diseases including infection and inflammation, lipid

metabolism, insulin resistance, liver diseases and iron uptake.[26–39] The *in vitro* iron overload models established to study such conditions are diverse with regards to (a) hepatic cell lines, (b) iron source and (c) iron treatment conditions. For example, Hirsh *et al.* eloquently highlight the differences in total iron concentrations in HepG2 and Hep3B cells in response to both transferrin-bound iron as well as non-transferrin bound iron.[36] This implies that concentration and source of iron is critical to understand how the cellular iron overload model will respond to iron loading. This may result in differences in cellular function and protein expression that could be imperative for downstream application. In addition, various groups have used multiple sources of iron ranging from citrate,-[26,29,31,36,37,39–44] nitriloacetate,-[28,35,43,45,46] and sulfate-[32,33,38,47,48] iron complexes with concentrations ranging from as low as 1 μM to as high as 10 mM, and also the treatment time varies as short as 4 hours to as long as 7 days[26,31–33,35–43,45–47,49,50] (see Supplementary Table S1 for detailed information). While it is difficult to directly compare these models, the iron concentration in the media required to load HepG2 cells with sufficient cellular iron and induce cytotoxicity seem to be depended on the type of iron source rather than the media concentration of iron itself. For instance, recently, Zibert and co-workers developed an iron overload model using HepG2 cells by treating them with around 10 mM of iron citrate ($Fe^{3+}$), iron sulfate ($Fe^{2+}$), and iron chloride ($Fe^{3+}$) for 4 h.[51] Although, cells were healthy up to 48 h, iron treatments for 4 h may not be a viable method for different studies. In another study, Sekine *et al.* monitored the cytocompatibility of Hep39b and Hepswx cells for six days in an iron overload model, treated with different concentrations of Fe-NTA, ranging from 30, 100, 300, 500 and 1000 μM. Except for 30 μM, the rest of the treatments showed significant toxicity comparted to non-treatment control.[28] As it is mentioned above, different iron sources have significant effect on iron loading. For instance, Barisani *et al.* used ferric ammonium citrate (~ 720 μM) to load HepG2 cells. In this model, cell toxicity was not observed up to 7 days.[32]

Consequently, the differences in iron source and treatment duration can introduce confound variables that may result in differences in measured outcomes impacting the comparison of these findings across studies in literature. This is best exemplified by Fang *et al.* and Petrak *et al.* who performed proteomic analysis HepG2 cells loaded with different concentrations of ferrous sulfate. They discovered that the expression of a number of proteins was sensitive to the iron concentration used.[32,33] This underlines the importance of having a consistent and reproducible *in vitro* iron overload model to study biology and evaluate therapeutics. Herein, we report the development of an iron overload HepG2 cell model, using ferric ammonium citrate, with a particular focus on the generation of ROS, and iron status with regards to labile and total iron.

# Methods

## Materials

Pierce Radioimmunoprecipitation assay (RIPA) lysis buffer, PBS buffer, Eagle's Minimum Essential Media (EMEM), Trypan blue, 2 mg/mL bovine serum albumin (BSA) standards, cell scrapers, and Pierce Coomassie (Bradford) protein assay kit were purchased from Thermo Fisher Scientific unless otherwise

mentioned. Fetal bovine serum, tissue culture treated 6-well and 48-well cell culture plates, tissue culture treated T25 flasks, concentrated nitric acid, ammonium acetate, ferric ammonium citrate (FAC), ferene (3-(2-Pyridyl)-5,6-di(2-furyl)-1,2,4-triazine-5',5"-disulfonic acid disodium salt), calcein acetoxymethl ester (Cal-AM) and sodium L-ascorbate were obtained from Sigma-Aldrich. 7-AAD solution was acquired from BioLegends. For cellular assay kits, both the DCFDA/H2DCFDA ROS generation kit (ab113851) and the JC-10 mitochondrial membrane potential assay kit (ab112134) were purchased from Abcam, while the MTT assay kit was purchased from ATCC (20-1010K).

### Cell culture

HepG2 cells, a hepatocarcinoma cell line (ATCC HB-8065), with passage numbers between 3 to 10 were used for all experiments. Cells were maintained in EMEM with media changed every 1–2 days. For all iron treatments, ferric ammonium citrate (FAC) was used as the source of iron (18 mole % iron). All concentrations were prepared with respect to iron in EMEM.

### Cell treatment with ferric ammonium citrate

For iron loading conditions, HepG2 cells were seeded in 6 wells plates at a density of 400,000 cells per well and grown for 2 days. Cells were treated with 1 mL media containing either 0, 50, 100, 200, 500 or 1000 μM iron from FAC each day for either 1 or 2 days. After iron loading, cells were washed with 1 mL PBS thrice. Cell lysates and subsequent total iron analysis were performed, as outlined below.

For iron retention conditions, HepG2 cells were seeded in 6 well plates at a density of 740,000 cells per well and grown for 2 days. Cells were then iron loaded by treating with 1 mL of 200 μM iron in media each day for 2 days. Then, cells were maintained for an additional 0, 1, 2 or 3 days in 1 mL of media without iron with the media replaced daily. Cells were washed with 1 mL PBS thrice. Cell lysates and subsequent total iron analysis were performed, as outlined below.

### Final protocol for establishing an iron overload HepG2 model

The final protocol for establishing an iron overload model in HepG2 was followed; cells were treated with iron-containing media each day for 2 days, followed by maintaining the cells in media without iron for 1 day.

### Iron overloading HepG2 cells

To assess changes in the iron overload model due to varying iron loading concentrations, cells were iron loaded with either 50, 100 or 200 μM of iron following the “Iron overloading HepG2 model” protocol. Prior to any analysis, cells were washed with PBS thrice.

For changes in total and labile iron, HepG2 cells were cultured at a density of 500,000 cells per T25 tissue culture flask. After following the iron overload model protocol, cell lysates were prepared and iron was quantified, as outline below. For changes in ROS generation and Calcein-based labile iron, HepG2 cells were cultured in 6 well plates at a density of 400,000 cells per well. Cells were stained and analyzed *via* flow cytometry, as described below. After being iron overloaded, HepG2 cells were also characterized for

their cellular functions including metabolic activity (see MTT assay), mitochondrial membrane potential (see JC-10 assay), membrane integrity (see Trypan Blue assay), and cell viability (see 7-AAD assay). For the MTT and JC-10 assay, cells were seeded in a 48 well plate at a density of 50,000 cells per well while for the Trypan blue and the 7-AAD assay, cells were cultured in 6 well plates at a density of 400,000 cells per well.

### Iron overload HepG2 cell culture and treatment with iron chelators

HepG2 cells were iron loaded with 50 μM following the “Iron overloading HepG2 model” protocol. After iron loading, cells were washed twice with PBS and then treated with 15 μM of iron chelators deferoxamine (DFO) or deferiprone (DFP) or deferasirox (DFX) prepared in EMEM for 48 hours. Cells were washed thrice with PBS and analyzed for ROS generation, changes in labile and total iron, and changes in transferrin receptor 1 expression – as outlined below. This experiment was done in triplicates. Non-iron loaded HepG2 cells were analyzed as negative control. Cells were seeded in 6 well plates at a density of 400,000 cells per well for each study.

### Cell lysate preparation and protein measurement

HepG2 cells were scraped and pelleted at 500 g for 5 minutes. Harvested cells were lysed in 300 μL Pierce RIPA buffer with sonication. Cell debris was pelleted, and the supernatants were quantitatively collected. Protein content was measured by Bradford assay. A standard curve was generated using BSA and sample concentrations were interpolated. Samples were kept at – 80°C prior to any further analysis.

### Iron quantification

A modified ferene assay was used to quantify both labile and total iron from cell lysates, as described elsewhere.[52] Iron standards were prepared from FAC in 4% nitric acid, ranging from 0 to 1000 μM.

### Labile iron measurement

Labile iron concentrations were determined from cell lysates prepared. 100 μL of cells lysates and 100 μL iron standards were transferred into clean Eppendorf tubes. To each, 100 μL ammonium acetate buffer (pH 4.5, 2.5 M) and 120 μL working solution (5 mM ferene and 10 mM ascorbic acid) were added and left overnight. This mixture was spun at 21,000 g for 10 minutes to pellet any insoluble salts and debris. Absorbance was read at 595 nm on a SpectraMax 190 Microplate Reader from Molecular Devices. Labile iron concentrations were interpolated from a standard curve generated by using iron standards.

### Total iron measurements

Total iron concentrations were determined from cell lysates by first digesting them with concentrated nitric acid maintained at 100 °C to 120 °C followed by resuspension of the dried acid-digested samples in 200 μL of 4% nitric acid. Iron standards (200 μL) were transferred into clean Eppendorf tubes. To each, 200 μL ammonium acetate buffer (pH 4.5, 2.5 M) and 240 μL working solution (5 mM ferene and 1 M

ascorbic acid) were added. This mixture was vortexed and left overnight. Absorbance was measured at 595 nm and sample concentrations were interpolated from the standard curves generated.

### ROS measurements

Cellular ROS generation measured using a DCFDA / H2DCFDA kit (Abcam 113851) on Beckman Coulters CytoFLEX Flow Cytometer. In short, DCFDA, a fluorogenic cell permeable dye, undergoes deacetylation by cellular esterases to a non-fluorescent dye. Cellular ROS oxidize this molecule into DCF which is highly fluorescent, detected in the FITC channel. Manufacturer's protocol was followed. In brief, after washing cells with PBS thrice, cells were stained with 5 µM DCFDA in EMEM and incubated for 20 minutes at 37 °C. Then, cells were washed with PBS, trypsinized and pelleted. At least 10,000 cells were analyzed via flow cytometry and DCF was measured by the 488 nm laser and the FITC emission filter (530/20 nm).

### Calcein-based labile iron measurements

Calcein acetoxymethyl ester (Cal-AM) was used to measure changes in the intracellular labile iron, described elsewhere.[53] Cal-AM is a non-fluorescent dye that readily permeates the cell membrane and is cleaved into calcein, which is fluorescent.[54,55] Calcein then binds to iron stoichiometrically which quenches its green fluorescence.[54,55] In short, cells were washed, tryspinized and pelleted at 500 g for 5 minutes. Cells were resuspended in PBS with 0.2 µM of Cal-AM and incubated for 20 minutes at room temperature. At least 10,000 cells were analyzed via flow cytometry and Calcein fluorescence was measured by the 488 nm laser and the FITC emission filter (530/20 nm).

### Metabolic activity by MTT assay

The MTT (3-(4,5-dimethylthiazolyl-2)-2,5-diphenyltetrazolium bromide) assay (ATCC 20-1010K) was performed according to manufacturer's protocol to investigate changes in metabolic activity. In brief, after iron loading, cells were treated with MTT for 2 hours followed by detergent-induced lysis for 4 hours. Absorbance was measured at 570 nm on SpectraMax 190 Microplate Reader from Molecular Devices. Cell viability was determined; ($mean_{570\ nm}$ treated cells / $mean_{570\ nm}$ untreated cells) x 100%.

### Mitochondrial membrane potential by JC-10 assay

The JC-10 mitochondrial membrane potential assay kit (abcam 112134) was performed, in accordance to manufacturer's protocol, to investigate changes in mitochondrial membrane potential. JC-10 localizes in the mitochondria and changes fluorescent emission from green to orange as membrane potential increases; its monomeric form, which emits at 520 nm, forms aggregates, which emits at 590 nm, as the mitochondria becomes more polarized. In brief, iron overload HepG2 cells were treated with JC-10 for 30 minutes at 37°C and fluorescence was measured at 490/525 and 540/590 (excitation/emission nm) on a SpectraMax 190 Microplate Reader from Molecular Devices. Mitochondrial membrane potential was determined as follows ((ratio of 520 nm / 590 nm in treated cells) / (ratio of 520 nm / 590 nm in control cells)) x 100%.

### Membrane integrity by Trypan blue exclusion assay

Membrane integrity was investigated using the trypan blue exclusion method, as described elsewhere.[56] In brief, iron overloaded cells were scraped and pelleted, then resuspended in media with trypan blue (HyClone Trypan Blue Stain – Fisher). Live and dead cells were counted using a hemocytometer and percentages were reported.

### Cell viability by 7-amino-actinomycin D (7-AAD) assay

Cell viability was determined with a cell impermeable 7-AAD (7-amino-actinomycin D) solution (BioLegend) that fluoresces upon binding to DNA. In other words, 7-AAD fluorescence is indicative of membrane damage. Manufacturer's protocol was followed. In short, iron overload cells were scraped and pelleted, then incubated with 5 µL of stock (50 µg / mL) per sample for 15 minutes at room temperature. Cells were then analyzed by flow cytometry; at least 10,000 cells were analyzed, and dead cells were gated in the APC channel (660/10 nm). Cell viabilities were reported as percentage of live cells (i.e., 7-AAD negative cells).

### Western blot analysis

Iron overload HepG2 cells were scarped, lysed, and protein concentrations were quantified as described above. Transferrin receptor 1 expression was investigated through western blots, as described elsewhere.[57] Proteins were separated in a 10% sodium dodecyl sulfate polyacrylamide gel and transferred to a nitrocellulose membrane. The membrane was blocked in 10% skim milk and incubated with both a monoclonal anti-transferrin receptor 1 (TfR1) antibody (H68.4 – Thermofischer) and GAPDH (Cell Signalling Technology) at 3 µg/mL overnight. Primary antibodies were fluorescently tagged through fluorescently labelled secondary antibodies; donkey anti-mouse with an infrared dye 700 (LI-COR) was incubated at 1:10,000 for 4 hours. The nitrocellulose membranes were imaged using LI-COR with resolution set at 169 µm, medium quality, 700 nm channel at intensity of 5, and scan area large enough to cover the membrane. The western blot was analyzed using LI-COR's Odyssey Application Software 3.0. Data was first normalized to the house keeping protein GAPDH, and then represented relative to the control cells; (ratio of TfR1:GAPDH in treated cells) / (ratio of TfR1:GAPDH in control cells).

## Results

### Establishing an iron overload HepG2 model

A protocol to establish an iron overload model for hepatocytes was developed using HepG2 cells and FAC as the source of non-transferrin bound iron (NTBI). First, the experimental conditions required to iron load HepG2 cells were explored (Fig. 1A & 1B). Cells were treated with varying concentrations of FAC for every 24 hours for either 24 hours or 48 hours resulting in significantly higher total cellular iron concentrations when compared to non-iron treated cells. 24-hour iron treatment resulted in 46.32 nmole iron /mg of protein ($p = 0.0005$), 43.89 nmole iron /mg of protein, ($p = 0.0009$), and 43.65 nmole iron /mg of protein

(p = 0.0009) respectively for 100, 200, and 1000 μM FAC treatment. 48-hour iron treatment further increased the cellular iron concentration in the range 76 to 84 nmole iron /mg of protein for all the treatment conditions and the values were significantly different from the control non-iron treated cells ($p < 0.0001$). Our data clearly show that cellular iron loading was dependent on the duration of the treatment rather than iron loading concentration. When comparing the different iron loading concentrations at either 24 hours or 48 hours, no significant difference is observed between 100, 200, or 1000 μM iron containing media. However, cells treated with 100, 200, and 1000 μM for 48 hours yielded significantly higher total iron concentrations than the cells treated for 24 hours ($p < 0.0001$, $p < 0.0001$, and $p < 0.0001$, respectively).

The duration of iron retention was investigated next (Fig. 1C). HepG2 cells were loaded with 200 μM every 24 hours for 48 hours. Then, these cells were maintained in fresh media for up to 3 days with media being replaced every day. Total iron concentrations did not change even up to 72-hour post-loading in fresh media. Taken together, to establish stable iron overload HepG2 cell model, cells were loaded with FAC every 24 hours for 48 hours followed by 24 hours of maintenance in fresh media.

### The effect of iron loading concentrations on cellular iron responses

Iron overload HepG2 cells were established using different iron loading concentrations (50, 100, and 200 μM) using the optimized protocol to investigate the changes in cellular response with respect to iron loading (Fig. 2) and cellular functions (Fig. 3). Key parameters examined in cellular iron responses including labile iron concentration (Fig. 2A and 2B), total iron concentration (Fig. 2C) and ROS generation (Fig. 2D). Iron loaded cells showed a concentration-dependent increase in the labile iron pool (LIP). There is a significant increase in the LIP quantified by the *u*-ferene assay when comparing non-loaded cells to cells loaded with 50 μM iron or cells loaded with 50 μM iron compared to 200 μM iron ($p = 0.0066$ and $p = 0.0010$, respectively). The dose-dependent increase in the LIP is further corroborated by the calcein-based fluorescent assay; calcein fluorescence reduces as it binds to labile or redox active iron. The significant reduction in calcein-based fluorescence between control cells and 50 μM iron overloaded cells and between 50 μM and 200 μM iron overloaded cells ($p = 0.0001$ and $p < 0.0001$, respectively) is suggestive of increasing labile iron concentrations.

Similar to iron loading investigations (Fig. 1A), there is an increase in total iron concentration (Fig. 2C) when cells are treated with 50, 100, and 200 μM of iron-containing media compared to controls ($p = 0.0165$, $p = 0.0030$ and $p = 0.0006$, respectively). Further, there is no appreciable differences in total iron loading amongst iron treated cells with different concentrations highlighting the reproducibility of establishing a HepG2-based iron overload cell model.

Interestingly, the concentration-dependent trend in labile iron concentrations is not observed for ROS generation (Fig. 2D). There was a significant increase in ROS mediated median fluorescence intensity when comparing non-iron loaded cells to iron loaded cells ($p = 0.0010$, $p = 0.0006$ and $p = 0.0006$ for cells loaded with 50, 100 and 200 μM iron, respectively). However, there was no significant differences when

comparing iron overloaded cells at any loading concentrations tested. Despite increasing labile iron concentrations, ROS generation does not increase with respect to increasing iron loading concentrations.

### Characterization of cellular functions in response to varying iron loading concentration

Cellular functions were characterized in iron overloaded HepG2 cells. Cell viability was measured as a function of either nuclear or plasma membrane integrity (Fig. 3A and 3B). In both cell viability assays, HepG2 cells loaded with 50 μM iron showed no significant differences when compared to control (non-iron loaded cells). Any iron loading concentrations above 100 μM yielded a significant increase in either nuclear or plasma membrane permeability when compared to controls ($p < 0.0001$ for all comparisons). Mitochondrial membrane potential was measured through the JC-10 assay, which takes advantage of the different fluorescent emissions when cells become apoptotic (Fig. 3C). HepG2 cells loaded with iron at 500 μM or 1000 μM had perturbed the mitochondrial membrane potential significantly when compared to the control ($p < 0.0001$ for both). No significant alterations in cells loaded with 50, 100 or 200 μM iron were observed. Metabolic activity was observed through the MTT assay which measures the rate of MTT conversion to formazan salt by intracellular enzymes, including dehydrogenase enzymes (Fig. 3D). All iron overloaded HepG2 cells yielded significantly lower metabolic activities when compared to the control ($p < 0.0001$ for all comparisons). Taken together, HepG2 cells loaded with 50 μM were similar to control cells with respect to nuclear membrane integrity, plasma membrane integrity and mitochondrial membrane potential. As iron loading concentrations increased, particularly at 200 μM or higher, cellular functions were significantly different to iron overload cells loaded with lower iron concentrations.

### Application of the iron overload model to investigate iron chelation in HepG2 cells

HepG2 cells loaded with 50 μM iron were treated with 15 μM DFO, DFX and DFP for 48 hours to investigate changes in iron concentrations, ROS, and protein expression. No changes were observed in cell viability with this treatment (Supplementary Fig. S1). All chelators showed significant reduction in iron concentrations after the treatment. DFO treated cells had a significant reduction in both LIP (Fig. 4A) and total iron concentrations ($p = 0.0154$ and $p = 0.0042$, respectively (Fig. 4B), DFX treated cells only had a significant reduction in LIP concentrations ($p = 0.0293$), and DFP treated cells only had a significant reduction in total iron concentrations ($p = 0.0340$) (Fig. 4A and 4B). Further, DFO and DFP reduced intracellular ROS generation when compared to untreated iron overload cells ($p < 0.0001$ and $p = 0.0283$, respectively). Interestingly, DFO treated cells showed ROS levels comparable to the non-iron loaded control cells. DFX showed no changes in ROS (Fig. 4C).

Transferrin receptor 1 (TfR1) expression was measured as cellular response to iron overload. Under iron overload conditions, TfR1 expression decreased when compared to control and iron overload HepG2 cells ($p < 0.0001$). Upon treatment with iron chelators significantly increased TfR1 expression when compared to iron overload cells ($p < 0.0001$). Interestingly, DFO and DFX treatment resulted in expression levels greater than non-iron loaded control cells (Fig. 4D).

# Discussion

In humans, all acquired iron, either TBI or NTBI, enters the liver where it is either stored, utilized or mobilized for systemic use.[6] As such, the liver is critical for coordinating iron homeostasis. An imbalance in this maintenance can result in iron overload where excess free iron results in hepatic toxicity and damage giving rise to a variety of disorders including hepatic insulin resistance,[11,12] fibrosis and cirrhosis,[13,14] and increased risk for hepatocellular carcinoma.[15,16] Therefore, *in vitro* hepatic iron overload models provide an invaluable tool to better understand pathogenesis whilst enabling the progression of treatment development. Such in vitro models exists, yet their utility is undermined by the extreme diversity in these studies, namely; (1) different hepatic cell lines, such has HepG2 versus Hep3B respond differently to NTBI, (2) various sources of NTBI are used, most commonly including citrate-[26,29,31,36,37,39–44], nitriloacetate-[28,35,43,45,46], and sulfate-[32,33,38,47,48] complexes, as well as other preparations[33,43,58,59], and (3) iron treatment vary greatly with vastly different concentrations and durations, ranging from as low as 1 µM to as high as 2 mM for as short as 6 hours to as long as 7 days[26,31–33,35–43,45–47,49,50]. A lack of consensus within the field can bias outcomes of interest. This is potentially highlighted in a proteomic study that investigated protein alterations in HepG2 cells loaded with two different iron concentrations; HepG2 cells treated with 10 µM resulted in 25 proteins being up-regulated and 5 proteins being down-regulated whereas HepG2 cells treated with 1000 µM resulted in 19 protein being up-regulated and 8 protein being down-regulated, with two down-regulated proteins at 10 µM becoming up-regulated at 1000 µM.[32,33] This motivated us to investigate this and establish a consistent iron overload *in vitro* model to enable reproducible findings.

HepG2 cells were loaded with iron from ferric ammonium citrate (FAC), a common complex in NTBI, to mimic iron accumulation in patients suffering from iron overload.[60–62] Whilst the uptake of NTBI has not been completely elucidated, NTBI is rapidly internalized by the hepatocytes via the DMT1 or the ZIP14 transmembrane metal-ion transporter.[20,26,63–65] Since iron treatment conditions vary greatly, HepG2 cells were first screened for changes in total iron with respect to concentration and duration of iron loading. Total iron in cells increased with the time of incubation rather than iron loading concentrations (Fig. 1); total iron concentrations were significantly more elevated in cells treated for 48 h compared to 24 h at the same concentrations, however, there were no significant differences between cells treated with different concentration for a given time. Total iron concentrations in loaded HepG2 cells were in the range of 75 to 85 nmole per mg protein (3.5 to 5.0 µg iron per mg protein) after 48 h incubation, which is in agreements with earlier reports.[36,50,66] This has been validated through ICP-MS, the gold standard approach for elemental analysis in our earlier report.[52] Taken together, 48 hour treatment periods is sufficient to induce iron overload, which is maintained for at least 3 days providing ample time to conduct further studies.

Next, we investigated the impact of iron loading concentrations using the established time stamps – load every 24 h for 48 h, followed by 24 h of fresh media. Intracellularly, a small fraction of redox labile iron is maintained in dynamic equilibrium such that it accounts for ~ 3–5% of the total iron.[67] This is observed using the *u*-ferene assay in control cells with 3.7% LIP (0.8 nmole of labile iron/mg of protein out of the

21.5 nmole of total iron/mg of protein). As shown in Fig. 1, HepG2 cells loaded with iron, irrespective of iron loading concentrations, showed no significant differences when comparing their total iron, highlighting the reproducibility of this iron overload model.

Moreover, similar to hepatic iron overload diseases, iron overloaded HepG2 cells demonstrate significantly elevated labile iron concentrations as iron loading concentrations increased. The labile iron concentration, using the *u*-ferene assay, were significantly increased when comparing control cells to iron overload HepG2 cells. This pattern was further corroborated with the calcein assay[45,47]. Elevated labile iron catalyzes the generation of ROS through the Haber-Weiss reaction, which imparts oxidative damage to lipids, proteins and DNA.[21,68,22,23,69] Intracellular ROS levels were measured and a significant increase was observed for iron overloaded cells. This increase in ROS has been documented in earlier reports.[28,31,32,38,45] Similar to total iron concentrations, ROS generation was not significantly different between cells treated with different iron loading concentrations. Huang *et al.* reports a linear correlation between lipid peroxidation and total iron concentrations, which might rationalize our findings.[38] While it is also possible that HepG2 cells have internal mechanisms to handle and maintain such high ROS levels, further work would need to validate this. In addition, iron overload cells treated with hydrogen peroxide further increased ROS generation ($p = 0.0024$) (Supplementary Fig. S2) demonstrating that the cells are susceptible to further ROS generation and that ROS generation is still within the assay's limit of detection. Taken together, using the established time stamps to develop an iron overload with different iron loading concentrations (50, 100 and 200 µM) only labile iron concentrations significantly changed.

Next, toxicity indicators were measured as a function of iron loading concentrations, lower iron loading concentrations better resembled non-iron loaded control cells in the measured cellular functions. As iron loading concentrations increased, iron overloaded HepG2 cells showed exacerbated decline in these parameters – as exemplified by HepG2 cells loaded with 1000 µM. Of importance, cytotoxicity indices vary greatly within literature. Abalea *et al.* report elevated LDH release in HepG2 cells treated with iron at 10 and 100 µM for 24 hours whilst Fang *et al.* report unchanged HepG2 cell proliferation for concentrations as high as 1000 µM treated for up to 5 days.[33,45] It is important to distinguish that both Abalea *et al.* and Fang *et al.* used nitriloacetate complexed iron. Different NTBI sources yield different kinetic parameters with regards to NTBI uptake.[43] Previous publications, using ferric ammonium citrate to treat HepG2 cells, also report varying toxicities. Parkes *et al.* report that nuclear membrane integrity changes at concentrations higher than 200 µM while LDH levels remain unchanged at concentrations as high as 1.4 mM.[43] In addition, Popovic *et al.* report that metabolic activity, measured by MTT, decreases below 80% of control only at concentrations exceeding 2 mM.[50] Given this variability and that many reports aim to investigate the treatment of iron overload or the reversal of ROS-mediated damage, it is essential that cytotoxic indices are thoroughly documented and account for different cellular parameters. Adopting this practice will empower reproducibility within the field. Our data showed that iron loading concentrations of 50 µM yield an iron overload model closest to control cells and that any concentration above 200 µM iron show significant alterations to cellular functions.

In order to assess the validity of this model, the response of iron overloaded HepG2 cells upon iron chelator treatment were investigated with regards labile and total iron within cells, ROS generation and TfR1 expression. A reduction in iron concentrations were observed, which is consistent with earlier reports.[38,43] Further, generation of intracellular ROS was also reduced with chelator treatment suggesting a protective action which is in accordance with Huang *et al.*'s report. Moreover, TfR1 expression was also modulated by changes in the cellular iron status.[38] TfR1 expression is regulated by iron regulatory proteins by binding to iron-responsive elements in the 3'-untranslated region of TfR1 mRNA transcripts such that there is decreased expression under iron overload conditions.[70] As such, TfR1 expression was reduced upon iron loading followed by a subsequent increase with chelator treatment. Such intracellular changes are observed elsewhere with both TfR1 and intracellular ferritin.[41] It is interesting to note that TfR1 expression were significantly higher for DFO and DFX treated cells when compared to non-iron overload control cells ($p < 0.0001$ for both chelators), as observed by Chenoufi *et al.*[41]

Taken together, we document the process to develop an iron overload HepG2 model for consistency and reproducibility within the field. There is a plethora of investigations into the consequences of hepatic iron overload on systemic dysregulation, however, existing in vitro iron overload models are undermined by the lack of consensus with regards to iron source, iron loading concentrations and iron treatment durations. We showed that HepG2 cells treated with 50 μM iron-enriched media every 24 h for 48 h, followed by maintenance in fresh media for 24 h establish an adequate iron overload model, as measured by changes in labile iron concentrations, total iron concentrations, ROS generation, indices of cytotoxicity, and protein expression. It is imperative to highlight the rigor for reproducibility in *in vitro* studies since these are often the frontline validation experiments that impact translation into *in vivo* investigations.

# Conclusions

We reported the development of an iron overload HepG2 cell model for the primary purpose of demonstrating the importance of being diligent about the iron source, iron treatment conditions and duration of the treatment. Iron loading cells with 50 μM of iron every 24 hours for 2 days, followed by maintenance for an additional 24 hours of in fresh media. In doing so, we demonstrated that only 50 μM iron is required to result in increased iron-dependent measured outcomes – ROS generation, labile iron and total iron concentrations. Moreover, 50 μM of iron was sufficiently mild enough to maintain cellular functions such that it closely resembled unloaded HepG2 cells. A robust protocol to establish iron overloading in HepG2 cells is of great importance as it highlights the current lack of consensus within the literature which translates into a lack of reproducibility with regards to iron-dependent measured outcomes and cellular functions. This process is adaptable to any other cell type.

# Declarations

**Acknowledgments:** The authors thank the Macromolecular Hub (CBR) for the use of their research facilities.

**Funding:** The authors acknowledge the funding by Canadian Institutes of Health Research (CIHR), Natural Sciences and Engineering Council of Canada (NSERC), and Canada Foundation for Innovation (CFI). JNK acknowledges the funding from NSERC-CREATE program. JNK acknowledges a Career Investigator Scholar award from the Michael Smith Foundation for Health Research (MSFHR). JNK is Tier 1 Canada Research Chair. SA acknowledges a MSFHR postdoctoral fellowship.

**Competing interests:** Authors declare no competing interests.

**Data and materials availability:** All data is available in the main text or the supplementary materials.

# References

1. Zhang, C. Essential functions of iron-requiring proteins in DNA replication, repair and cell cycle control. Protein Cell **5**, 750–760 (2014).
2. Sheftel, A. D. *et al.* Human Ind1, an Iron-Sulfur Cluster Assembly Factor for Respiratory Complex I. Mol. Cell. Biol. **29**, 6059–6073 (2009).
3. Lane, D. J. R. *et al.* Cellular iron uptake, trafficking and metabolism: Key molecules and mechanisms and their roles in disease. Biochim. Biophys. Acta BBA - Mol. Cell Res. **1853**, 1130–1144 (2015).
4. Mulaikal, T. A. & Emond, J. C. Physiology and Anatomy of the Liver. in *Liver Anesthesiology and Critical Care Medicine* (ed. Wagener, G.) 3–20 (Springer, 2012).
5. Racanelli, V. & Rehermann, B. The liver as an immunological organ. Hepatol. Baltim. Md **43**, S54-62 (2006).
6. Anderson, E. R. & Shah, Y. M. Iron homeostasis in the liver. Compr. Physiol. **3**, 315–330 (2013).
7. Sakurada, A. *et al.* An intronic single nucleotide polymorphism in the MUTYH gene is associated with increased risk for HCV-induced hepatocellular carcinoma. Free Radic. Biol. Med. **129**, 88–96 (2018).
8. Bonkovsky, H. L. Iron and the liver. Am J Med Sci **301**, 32–43 (1991).
9. Aigner, E. *et al.* Pathways underlying iron accumulation in human nonalcoholic fatty liver disease. Am. J. Clin. Nutr. **87**, 1374–1383 (2008).
10. Bozzini, C. *et al.* Prevalence of body iron excess in the metabolic syndrome. Diabetes Care **28**, 2061–2063 (2005).
11. Britton, L. *et al.* Hepatic iron concentration correlates with insulin sensitivity in nonalcoholic fatty liver disease. Hepatol. Commun. **2**, 644–653 (2018).
12. Fargion, S. *et al.* Iron and insulin resistance. Aliment. Pharmacol. Ther. **22**, 61–63 (2005).
13. Pietrangelo, A. *et al.* Enhanced hepatic collagen type I mRNA expression into fat-storing cells in a rodent model of hemochromatosis. Hepatol. Baltim. Md **19**, 714–721 (1994).
14. Ramm, G. A. & Ruddell, R. G. Hepatotoxicity of Iron Overload: Mechanisms of Iron-Induced Hepatic Fibrogenesis. Semin. Liver Dis. **25**, 433–449 (2005).

15. Borgna-Pignatti, C. *et al.* Hepatocellular carcinoma in the thalassaemia syndromes. Br. J. Haematol. **124**, 114–117 (2004).
16. Bradbear, R. A. *et al.* Cohort study of internal malignancy in genetic hemochromatosis and other chronic nonalcoholic liver diseases. J. Natl. Cancer Inst. **75**, 81–84 (1985).
17. Jacobs, A. An intracellular transit iron pool. *Ciba Found. Symp.* 91–106 (1976)
18. Jacobs, A. Low molecular weight intracellular iron transport compounds. Blood **50**, 433–439 (1977).
19. Cabantchik, Z. I. Labile iron in cells and body fluids: physiology, pathology, and pharmacology. Front. Pharmacol. **5**, (2014).
20. Le Lan, C. *et al.* Redox active plasma iron in C282Y/C282Y hemochromatosis. Blood **105**, 4527–4531 (2005).
21. Kehrer, J. P. The Haber–Weiss reaction and mechanisms of toxicity. Toxicology **149**, 43–50 (2000).
22. Anderson, G. J. Mechanisms of iron loading and toxicity. Am. J. Hematol. **82**, 1128–1131 (2007).
23. Eaton, J. W. & Qian, M. Molecular bases of cellular iron toxicity. Free Radic. Biol. Med. **32**, 833–840 (2002).
24. Nurtjahja-Tjendraputra, E., Fu, D., Phang, J. M. & Richardson, D. R. Iron chelation regulates cyclin D1 expression via the proteasome: a link to iron deficiency-mediated growth suppression. Blood **109**, 4045–4054 (2007).
25. Kempe, D. S. *et al.* Enhanced programmed cell death of iron-deficient erythrocytes. FASEB J. Off. Publ. Fed. Am. Soc. Exp. Biol. **20**, 368–370 (2006).
26. Nam, H. *et al.* ZIP14 and DMT1 in the liver, pancreas, and heart are differentially regulated by iron deficiency and overload: implications for tissue iron uptake in iron-related disorders. Haematologica **98**, 1049–1057 (2013).
27. Villarroel, P., Le Blanc, S. & Arredondo, M. Interleukin-6 and Lipopolysaccharide Modulate Hepcidin mRNA Expression by Hepg2 Cells. Biol. Trace Elem. Res. **150**, 496–501 (2012).
28. Sekine, S. *et al.* Mitochondrial iron accumulation exacerbates hepatic toxicity caused by hepatitis C virus core protein. Toxicol. Appl. Pharmacol. **282**, 237–243 (2015).
29. Parkes, J. G. & Templeton, D. M. Modulation of stellate cell proliferation and gene expression by rat hepatocytes: effect of toxic iron overload. Toxicol. Lett. **144**, 225–233 (2003).
30. Dongiovanni, P. *et al.* High Fat Diet Subverts Hepatocellular Iron Uptake Determining Dysmetabolic Iron Overload. PLOS ONE **10**, e0116855 (2015).
31. Barisani, D., Meneveri, R., Ginelli, E., Cassani, C. & Conte, D. Iron overload and gene expression in HepG2 cells: analysis by differential display. FEBS Lett. **469**, 208–212 (2000).
32. Petrak, J. *et al.* Proteomic analysis of iron overload in human hepatoma cells. Am. J. Physiol.-Gastrointest. Liver Physiol. **290**, G1059–G1066 (2006).
33. Fang, C., Zhao, C., Liu, X., Yang, P. & Lu, H. Protein alteration of HepG2.2.15 cells induced by iron overload. PROTEOMICS **12**, 1378–1390 (2012).

34. Mehta, K. *et al.* Characterization of hepcidin response to holotransferrin in novel recombinant TfR1 HepG2 cells. Blood Cells. Mol. Dis. **61**, 37–45 (2016).
35. Gao, J., Zhao, N., Knutson, M. D. & Enns, C. A. The Hereditary Hemochromatosis Protein, HFE, Inhibits Iron Uptake *via* Down-regulation of Zip14 in HepG2 Cells. J. Biol. Chem. **283**, 21462–21468 (2008).
36. Hirsh, M., Konijn, A. M. & Iancu, T. C. Acquisition, storage and release of iron by cultured human hepatoma cells. J. Hepatol. **36**, 30–38 (2002).
37. Guillemot, J., Asselin, M.-C., Susan-Resiga, D., Essalmani, R. & Seidah, N. G. Deferoxamine stimulates LDLR expression and LDL uptake in HepG2 cells. Mol. Nutr. Food Res. **60**, 600–608 (2016).
38. Huang, X. *et al.* Ferrous ion autoxidation and its chelation in iron-loaded human liver HepG2 cells. Free Radic. Biol. Med. **32**, 84–92 (2002).
39. Cragg, L. *et al.* The iron chelator L1 potentiates oxidative DNA damage in iron-loaded liver cells. Blood **92**, 632–638 (1998).
40. Rakba, N. *et al.* Antiproliferative and apoptotic effects of O-Trensox, a new synthetic iron chelator, on differentiated human hepatoma cell lines. Carcinogenesis **21**, 943–951 (2000).
41. Chenoufi, N. *et al.* Antiproliferative effect of deferiprone on the Hep G2 cell line. Biochem. Pharmacol. **56**, 431–437 (1998).
42. Barnum-Huckins, K. & Adrian, G. S. Iron regulation of transferrin synthesis in the human hepatoma cell line HEPG2. Cell Biol. Int. **24**, 71–77 (2000).
43. Parkes, J. G., Randell, E. W., Olivieri, N. F. & Templeton, D. M. Modulation by iron loading and chelation of the uptake of non-transferrin-bound iron by human liver cells. Biochim. Biophys. Acta **1243**, 373–380 (1995).
44. Popovic, Z. & Templeton, D. M. Iron accumulation and iron-regulatory protein activity in human hepatoma (HepG2) cells. Mol. Cell. Biochem. **265**, 37–45 (2004).
45. Abalea, V. *et al.* Iron-induced oxidative DNA damage and its repair in primary rat hepatocyte culture. Carcinogenesis **19**, 1053–1059 (1998).
46. Lymboussaki, A. *et al.* The role of the iron responsive element in the control of ferroportin1/IREG1/MTP1 gene expression. J. Hepatol. **39**, 710–715 (2003).
47. Ali, A., Zhang, Q., Dai, J. & Huang, X. Calcein as a fluorescent iron chemosensor for the determination of low molecular weight iron in biological fluids. Biometals **16**, 285–293 (2003).
48. Teixeira, J. *et al.* Development of a Mitochondriotropic Antioxidant Based on Caffeic Acid: Proof of Concept on Cellular and Mitochondrial Oxidative Stress Models. J. Med. Chem. **60**, 7084–7098 (2017).
49. Sturm, B., Goldenberg, H. & Scheiber-Mojdehkar, B. Transient increase of the labile iron pool in HepG2 cells by intravenous iron preparations. Eur. J. Biochem. **270**, 3731–3738 (2003).
50. Popovic, Z. & Templeton, D. M. Iron accumulation and iron-regulatory protein activity in human hepatoma (HepG2) cells. Mol. Cell. Biochem. **265**, 37–45 (2004).

51. Guttmann, S. *et al.* Compound-specific adaptation of hepatoma cell lines to toxic iron. Metallomics **11**, 1836–1846 (2019).
52. Abbasi, U., Abbina, S., Gill, A., Bhagat, V. & Kizhakkedathu, J. N. A facile colorimetric method for the quantification of labile iron pool and total iron in cells and tissue specimens. Sci. Rep. **11**, 6008 (2021).
53. Breuer, W., Epsztejn, S. & Cabantchik, Z. I. Iron Acquired from Transferrin by K562 Cells Is Delivered into a Cytoplasmic Pool of Chelatable Iron(II). J. Biol. Chem. **270**, 24209–24215 (1995).
54. Tenopoulou, M., Kurz, T., Doulias, P.-T., Galaris, D. & Brunk, U. T. Does the calcein-AM method assay the total cellular 'labile iron pool' or only a fraction of it? Biochem. J. **403**, 261–266 (2007).
55. Thomas, F. *et al.* Calcein as a Fluorescent Probe for Ferric Iron application to iron nutrition in plant cells. J. Biol. Chem. **274**, 13375–13383 (1999).
56. Strober, W. Trypan Blue Exclusion Test of Cell Viability. *Curr. Protoc. Immunol.* **21**, A.3B.1-A.3B.2 (1997).
57. Hubert, N. *et al.* Regulation of ferritin and transferrin receptor expression by iron in human hepatocyte cultures. J. Hepatol. **18**, 301–312 (1993).
58. Lewandowska, H. *et al.* LDL dinitrosyl iron complex: A new transferrin-independent route for iron delivery in hepatocytes. BioFactors Oxf. Engl. **44**, 192–201 (2018).
59. Sturm, B., Goldenberg, H. & Scheiber-Mojdehkar, B. Transient increase of the labile iron pool in HepG2 cells by intravenous iron preparations. Eur. J. Biochem. **270**, 3731–3738 (2003).
60. Faller, B. & Nick, H. Kinetics and Mechanism of Iron(III) Removal from Citrate by Desferrioxamine B and 3-Hydroxy-1,2-Dimethyl-4-Pyridone. J. Am. Chem. Soc. **116**, 3860–3865 (1994).
61. Grootveld, M. *et al.* Non-transferrin-bound iron in plasma or serum from patients with idiopathic hemochromatosis. Characterization by high performance liquid chromatography and nuclear magnetic resonance spectroscopy. J. Biol. Chem. **264**, 4417–4422 (1989).
62. Evans, R. W. *et al.* Nature of non-transferrin-bound iron: studies on iron citrate complexes and thalassemic sera. JBIC J. Biol. Inorg. Chem. **13**, 57–74 (2008).
63. Brissot, P., Wright, T. L., Ma, W. L. & Weisiger, R. A. Efficient clearance of non-transferrin-bound iron by rat liver. Implications for hepatic iron loading in iron overload states. J. Clin. Invest. **76**, 1463–1470 (1985).
64. Randell, E. W., Parkes, J. G., Olivieri, N. F. & Templeton, D. M. Uptake of non-transferrin-bound iron by both reductive and nonreductive processes is modulated by intracellular iron. J. Biol. Chem. **269**, 16046–16053 (1994).
65. Pinilla-Tenas, J. J. *et al.* Zip14 is a complex broad-scope metal-ion transporter whose functional properties support roles in the cellular uptake of zinc and nontransferrin-bound iron. Am. J. Physiol. Cell Physiol. **301**, C862-871 (2011).
66. Ternes, N., Scheiber-Mojdehkar, B., Landgraf, G., Goldenberg, H. & Sturm, B. Iron availability and complex stability of iron hydroxyethyl starch and iron dextran—a comparative in vitro study with liver

cells and macrophages. Nephrol. Dial. Transplant. **22**, 2824–2830 (2007).

67. Kruszewski, M. Labile iron pool: the main determinant of cellular response to oxidative stress. Mutat. Res. **531**, 81–92 (2003).
68. Koppenol, W. H. The Haber-Weiss cycle – 70 years later. Redox Rep. **6**, 229–234 (2001).
69. Richardson, D. R. Molecular mechanisms of iron uptake by cells and the use of iron chelators for the treatment of cancer. Curr. Med. Chem. **12**, 2711–2729 (2005).
70. Hentze, M. W., Muckenthaler, M. U., Galy, B. & Camaschella, C. Two to Tango: Regulation of Mammalian Iron Metabolism. Cell **142**, 24–38 (2010).
71. Li, S.-W. *et al.* Iron overload induced by ferric ammonium citrate triggers reactive oxygen species-mediated apoptosis via both extrinsic and intrinsic pathways in human hepatic cells. Hum. Exp. Toxicol. **35**, 598–607 (2016).
72. Karim, A. *et al.* Iron Overload Induces Oxidative Stress, Cell Cycle Arrest and Apoptosis in Chondrocytes. *Front. Cell Dev. Biol.* **10**, (2022).

# Figures

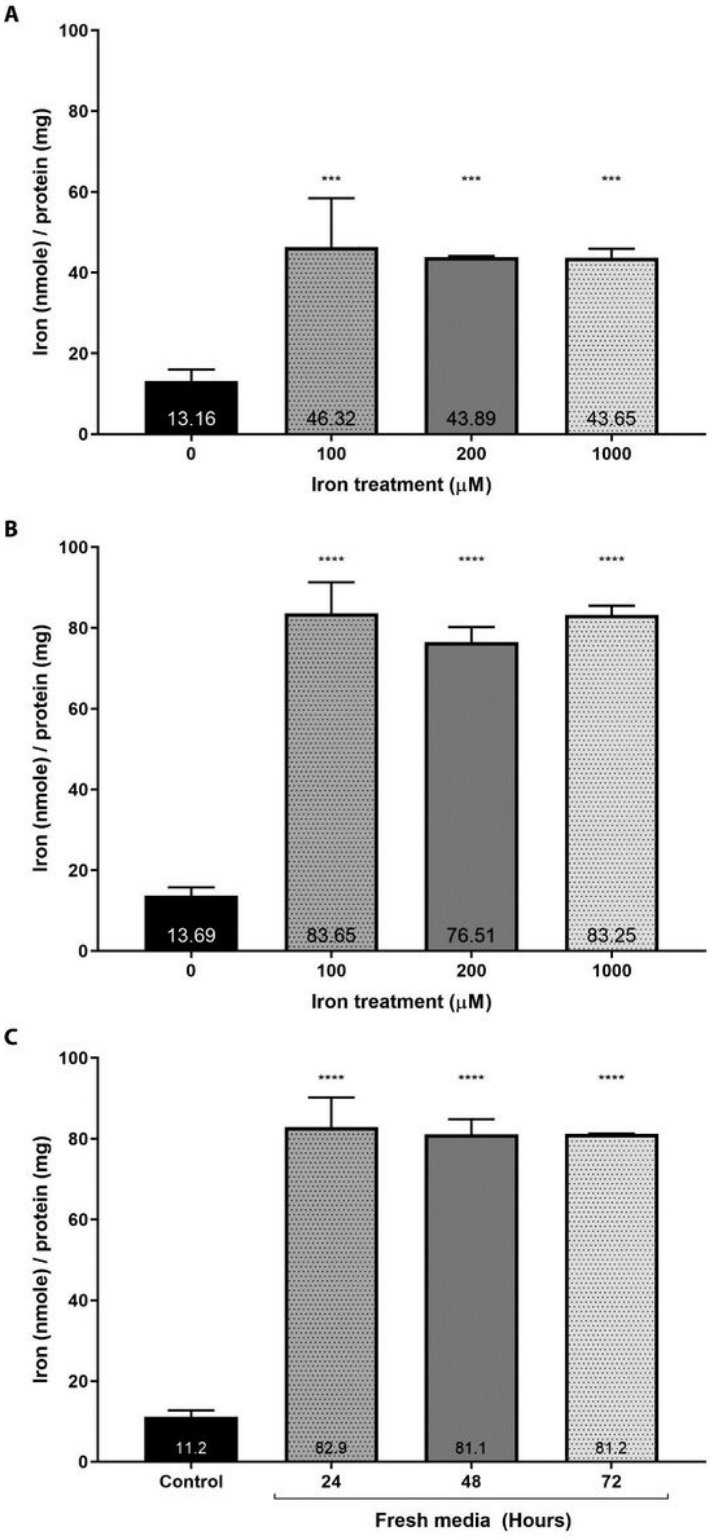


## Figure 1

**The effect of iron concentration and treatment time on establishing an iron overload HepG2 cell model.** (**A** & **B**) HepG2 cells were treated with varying concentrations of iron (100 to 1000 μM) in the form of FAC either once in 24 hours (**A**) or twice in 48 hours (**B**). (**C**) HepG2 cells were first treated with 200 μM every 24 hours for 48 hours. Then, these cells were maintained in fresh media without iron for up to 72 hours with media being changed every 24 hours. Total iron was analyzed using *u*-ferene assay.[52] Error bars

show standard deviations for N = 3 independent replicates. One-way ANOVA with Dunnett's correction method were performed to compare differences against the control or non-iron overloaded cells. One-way ANOVA with Sidak's correction method was performed to compare the iron loading with 24 hour or 48-hour treatment. **** represent $p < 0.0001$ and *** represents $p < 0.0010$. All statistical analysis were performed using GraphPad Prism.

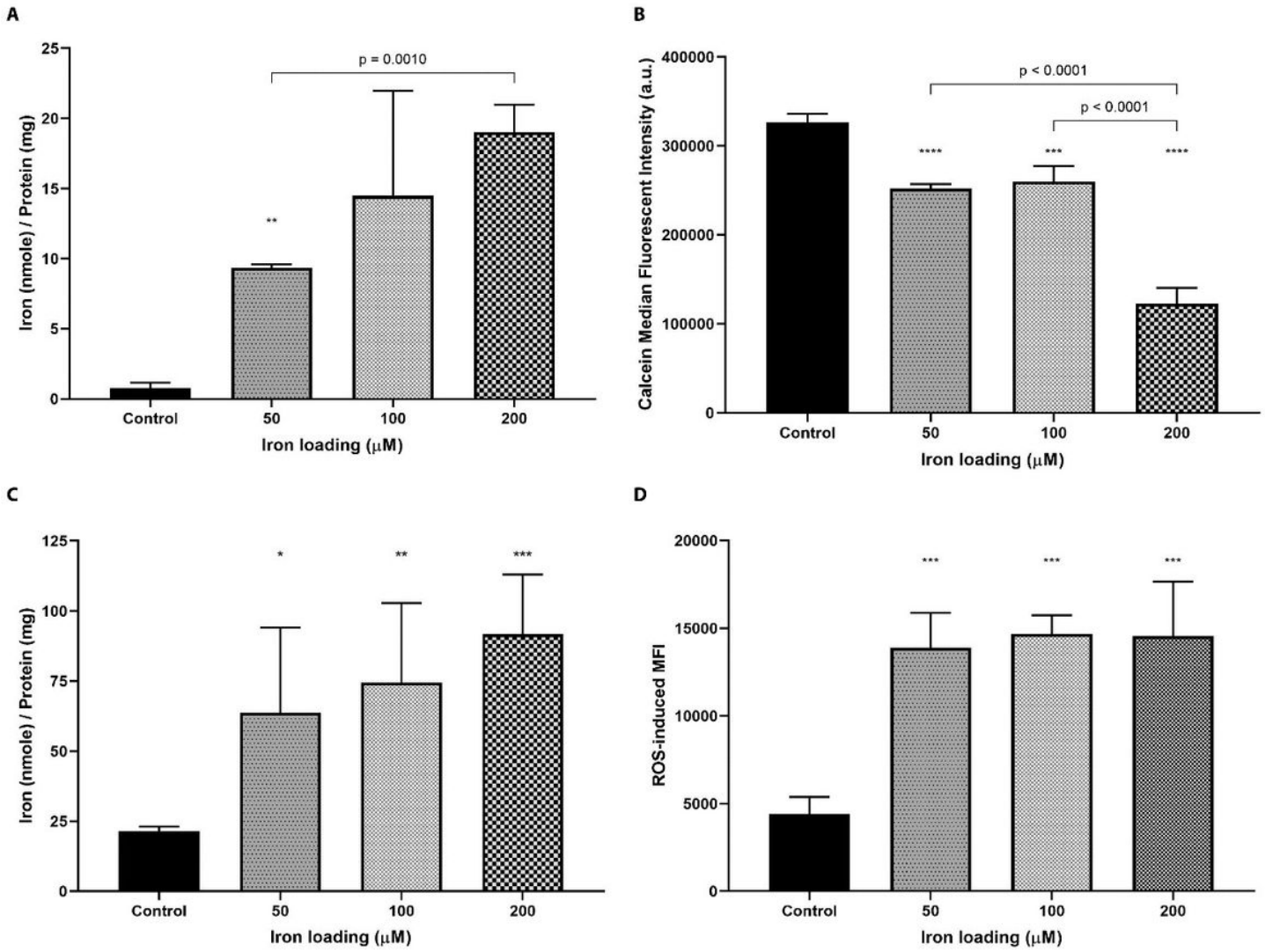


## Figure 2

**The effect of varying iron loading concentrations (50 to 200 μM) on labile iron, total iron and the generation of reactive oxidative species (ROS) in HepG2 cells.** (**A**) Labile iron was quantified using the *u*-ferene assay. One-way ANOVA with Sidak's correction method was used to compare iron-loaded cells with control cells. (**B**) Changes in the intracellular labile iron pool was monitored *via* fluorescence. Calcein fluorescence is quenched in the presence of iron. One-way ANOVA with either Sidak's or Dunnett's correction method was used to compare iron loaded cells with control cells. (**C**) Total iron was quantified using the *u*-ferene assay. One-way ANOVA with Dunnett's correction method was used to compare iron loaded cells with control cells. (**D**) ROS generation was measured using a DCFDA/DCF ROS kit in at least

10,000 HepG2 cells *via* flow cytometry. One-way ANOVA with Dunnett's correction method was used to compare iron loaded cells with control cells. Error bars show standard deviations for N = 3 independent replicates. Statistical analyses were performed using GraphPad Prism. **** represent p < 0.0001, *** represents p < 0.0010, ** represents p < 0.0100 and * represents p < 0.05.

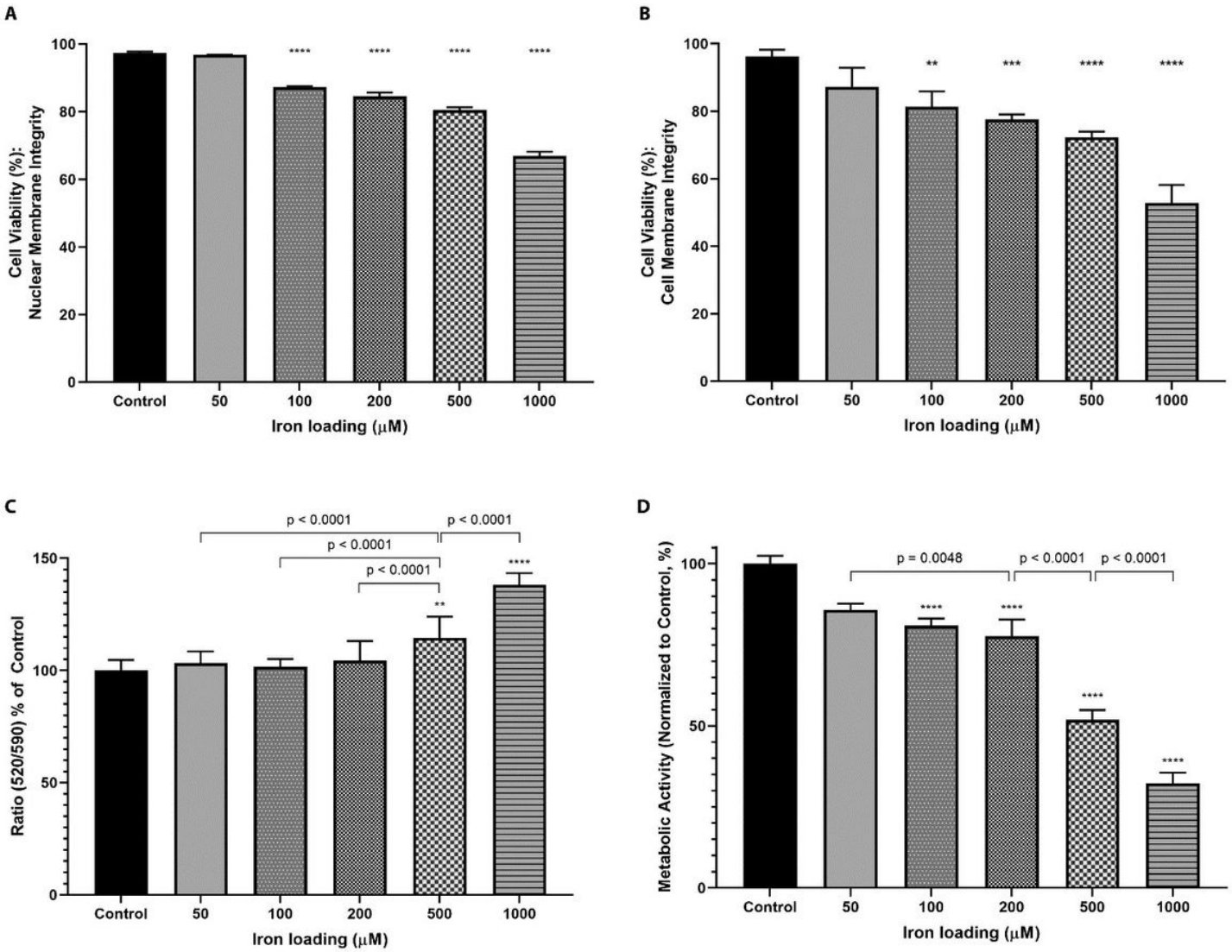


## Figure 3

**Characterization of cellular functions of HepG2 cells loaded with varying iron concentrations (50 to 200 μM).** (**A**) Cell viability was measured using a membrane impermeable 7-aminoactinomycin D (7-AAD) *via* a flow cytometry, analyzing at least 10,000 cells. 7-AAD binds to DNA and the fluorescence is detected in PC5.5 channel (710/50 nm). One-way ANOVA with Dunnett's correction method were performed to compare iron loaded cells with control cells. (**B**) Cell membrane integrity was measured using the Trypan blue (TB) exclusion assay. This dye is membrane impermeable. Cells with or without TB uptake were counted using a hemocytometer. One-way ANOVA with Dunnett's correction method were performed to compare iron-loaded cells with control cells. (**C**) Mitochondrial membrane potential was measured using the JC-10 assay kit using a plate reader. The ratio of fluorescence emitted at 590 nm and 540 nm were

normalized to control cells. One-way ANOVA with Dunnett's correction method were performed to compare iron loaded cells with control cells. Similarly, one-way ANOVA with Dunnett's correction method were performed to compare iron loaded cells with cells loaded with 500 μM. (**D**) Metabolic activity was measured using the MTT assay using a plate reader. One-way ANOVA with Dunnett's correction method were performed to compare iron loaded cells with control cells. One way ANOVA with Tukey's correction was also performed to compare different iron loaded cells with each other. Error bars show standard deviations for 3–6 independent replicates. All statistical analysis were performed using GraphPad Prism. **** represents $p < 0.0001$, *** represents $p < 0.0010$, and ** represents $p < 0.0100$.

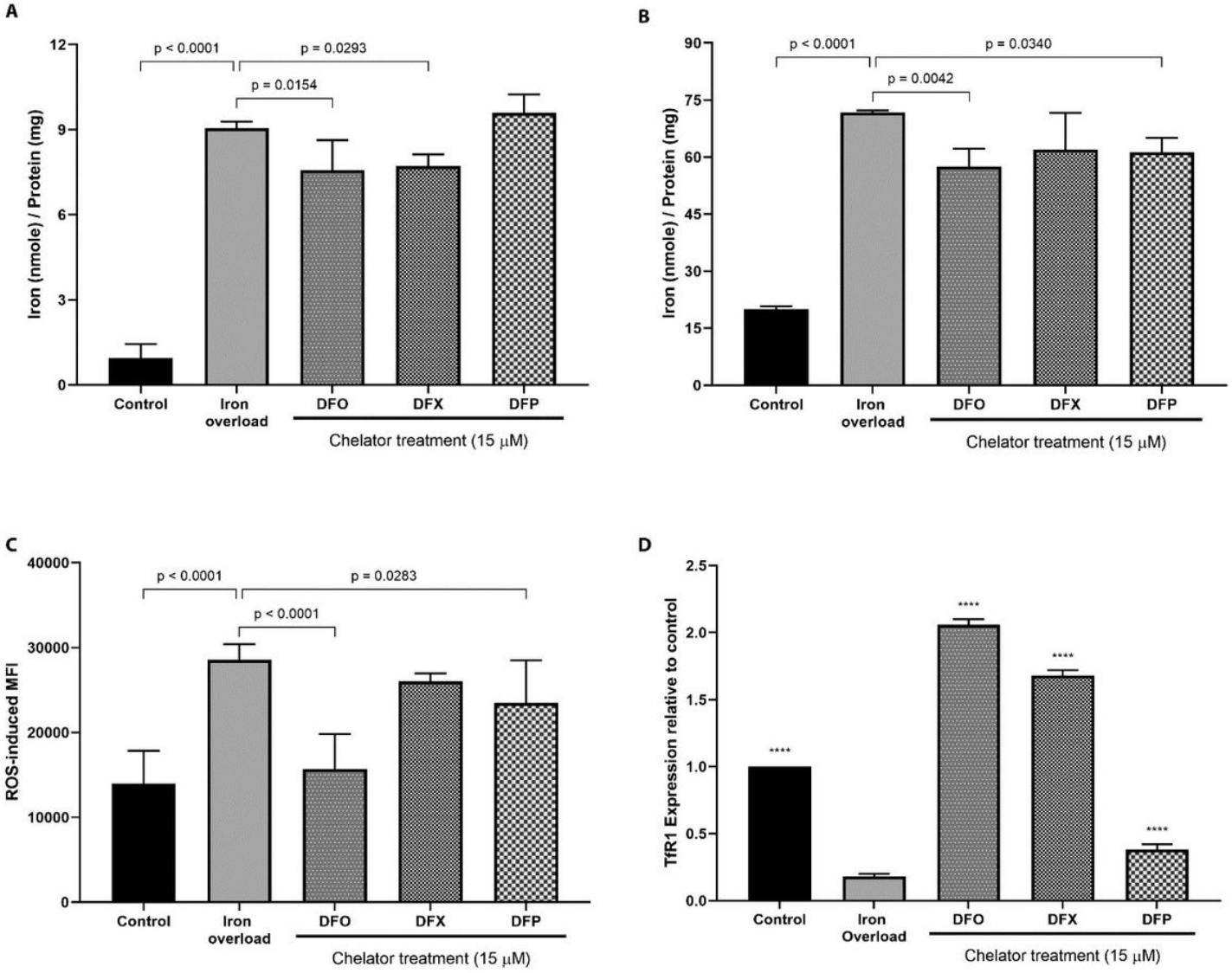


## Figure 4

**Effect of iron chelation in iron overload HepG2 cells.** Labile iron (**A**) and total iron (**B**) were quantified using the *u*-ferene assay. (**C**) ROS generation was measured using a DCFDA/DCF ROS kit in at least 10,000 cells *via* flow cytometry. (**D**) Relative expression of TfR1, normalized to control cells, were measured using western blot and quantified using LI-COR's Odyssey Software Application. HepG2 cells were loaded with 50 μM following the established protocol. Error bars show standard deviations for N = 3

independent replicates. One-way ANOVA with Dunnett's correction method were performed to compared iron overloaded cells with the either control or chelator treated cells. Statistical analyses were preformed using GraphPad Prism. **** represents $p < 0.0001$.

## Supplementary Files

This is a list of supplementary files associated with this preprint. Click to download.

- Supportingfiguresandtables.docx